

Properties and Reactivity Patterns of AsP₃: An Experimental and Computational Study of Group 15 Elemental Molecules

Brandi M. Cossairt and Christopher C. Cummins*

Massachusetts Institute of Technology, Department of Chemistry, 77 Massachusetts Avenue, Cambridge, Massachusetts 02139

Received August 5, 2009; E-mail: ccummins@mit.edu

Abstract: Facile synthetic access to the isolable, thermally robust AsP₃ molecule has allowed for a thorough study of its physical properties and reaction chemistry with a variety of transition-metal and organic fragments. The electronic properties of AsP₃ in comparison with P₄ are revealed by DFT and atoms in molecules (AIM) approaches and are discussed in relation to the observed electrochemical profiles and the phosphorus NMR properties of the two molecules. An investigation of the nucleus independent chemical shifts revealed that AsP₃ retains spherical aromaticity. The thermodynamic properties of AsP₃ and P₄ are described. The reaction types explored in this study include the thermal decomposition of the AsP₃ tetrahedron to its elements, the synthesis and structural characterization of [(AsP₃)FeCp*(dippe)][BPh₄] (dippe = 1,2-bis(diphenylphosphino)ethane), **1**, selective single As-P bond cleavage reactions, including the synthesis and structural characterization of AsP₃(P(N(ⁱPr)₂)N(SiMe₃)₂)₂, **2**, and activations of AsP₃ by reactive early transition-metal fragments including Nb(H)(η^2 -^tBu(H)C=NAr)(N[CH₂^tBu]Ar)₂ and Mo(N[^tBu]Ar)₃ (Ar = 3,5-Me₂C₆H₃). In the presence of reducing equivalents, AsP₃ was found to allow access to [Na][E₃Nb(ODipp)₃] (Dipp = 2,6-diisopropylphenyl) complexes (E = As or P) which themselves allow access to mixtures of As_nP_{4-n} ($n = 1-4$).

Introduction

White phosphorus, P₄, is of interest as a soluble, molecular form of this element obtained industrially via the thermal method of phosphate rock reduction. P₄ is the primary precursor to most P-containing compounds.¹ Melting without decomposition at 44 °C, pure P₄ is a white, waxy substance that presents no difficulties in terms of isolation, storage, and handling, as long as oxygen is excluded.^{1,2} On the other hand, yellow arsenic, As₄, is thermally and photochemically unstable in the condensed phase, reverting readily to the metallic form.² As such, its chemistry and application in industry is not well developed. Recently, the interpnictide molecule AsP₃ was synthesized in pure form and was shown to be robust, isolable, and as easy to handle as P₄ itself.³

Though only recently isolated and studied as a pure material, AsP₃ has long been contemplated by inorganic chemists in both academic and industrial settings. Ozin was the first to observe AsP₃ as one component of a hot, gas-phase mixture of arsenic and phosphorus vapors using Raman spectroscopy, inspiring chemists to speculate on the stability of the AsP₃ heteroatomic tetrahedron.⁴ The physical properties of solid and liquid arsenic-phosphorus phases have been described in some detail,^{5,6} but our understanding of the nature and properties of

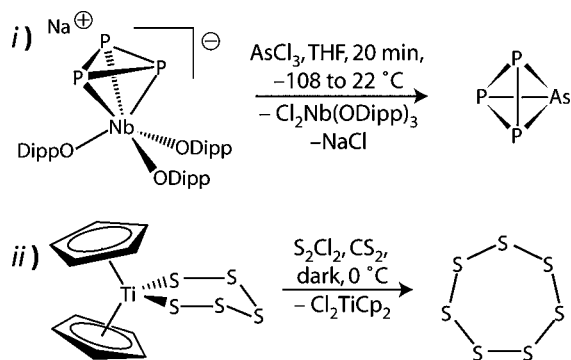
the tetraatomic tetrahedra As_nP_{4-n} ($n = 1-3$) is far from complete. AsP₃ has been suggested as an impurity in white phosphorus as prepared industrially.⁷ The apatite mineral used in the industrial production of P₄ is known to contain a small percentage of As for P substitution (0.003–0.03%) which is not removed prior to reduction and likely leads to some amount of AsP₃ impurity in industrially prepared P₄.^{8,9} With our discovery of a selective, niobium-mediated synthesis of AsP₃ and the present work, we are elucidating both the physical and chemical properties of this small molecule that bridges the gap between the soluble, molecular forms of the elements phosphorus and arsenic.

The present work delivers an overview of the synthesis and properties of AsP₃ as well as a detailed picture of the structural and electronic properties of AsP₃ as deduced by experiment, density functional theory (DFT),¹⁰ and Bader's atoms in molecules (AIM)¹¹ analysis. Also described herein are reactivity studies of AsP₃ with transition-metal complexes and with main-group element systems, for comparison with related data on P₄

- (1) Emsley, J. *The 13th element: the sordid tale of murder, fire and phosphorus*; John Wiley & Sons, Inc.: New York, 2000.
- (2) Greenwood, N. N.; Earnshaw, A. *Chemistry of the Elements*, 2nd ed.; Butterworth-Heinemann: Oxford, 1997.
- (3) Cossairt, B. M.; Diawara, M. C.; Cummins, C. C. *Science* **2009**, *323*, 602.
- (4) Ozin, G. A. *J. Chem. Soc. A* **1970**, 2307–2310.
- (5) Karakaya, I.; Thompson, W. T. *J. Phase Equilib.* **1991**, *12*, 343–346.

- (6) Ugai, Y. A.; Semenova, G. V.; Berendt, E.; Goncharov, E. G. *Russ. J. Phys. Chem.* **1979**, *53*, 576–577.
- (7) Schipper, W. Research and Development, Thermphos International. Personal communication.
- (8) Stow, S. H. *Econ. Geol.* **1969**, *64*, 667–671.
- (9) Harnisch, H.; Heymer, G.; Klose, W.; Schroder, K. In *Winnacker-Kuchler: Chemische Technik: Prozesse und Produkte*; Dittmeyer, R., Keim, W., Kreysa, G., Oberholz, A., Eds.; Wiley-VCH: Weinheim, 2005; Vol. 3, pp 343–427.
- (10) te Velde, G.; Bickelhaupt, F. M.; Baerends, E. J.; Fonseca Guerra, C.; van Gisbergen, S. J. A.; Snijders, J. G.; Ziegler, T. *J. Comput. Chem.* **2001**, *22*, 931–967.
- (11) Bader, R. F. W. *Atoms in Molecules: A Quantum Theory*; Oxford University Press: New York, 1994.

Scheme 1



reactivity, and to show that under the proper conditions, AsP_3 serves as a soluble As^0 source. The utility of AsP_3 for the synthesis of mixed arsenic–phosphorus ligands that would be difficult to synthesize by other means will also be highlighted.

Results and Discussion

Synthesis and Physical Properties of AsP_3 . The industrial synthesis of elemental phosphorus has remained essentially unchanged for over a century and consists of heating phosphate rock in excess of 1400 °C with coke and gravel.^{1,9} White phosphorus can also be prepared from red phosphorus by thermolysis at elevated temperature, similar to the synthesis of yellow arsenic from metallic arsenic.² White phosphorus has become difficult to obtain for research purposes in the United States, and both white and red phosphorus are classified by the DEA as List I federally regulated substances.¹²

Anionic *cyclo*- P_3 complexes of niobium have proven to be effective as P_3^{3-} transfer agents, and when combined with an E^{3+} source ($\text{E} = \text{P}, \text{As}, \text{Sb}$), we have shown that access to P_4 , AsP_3 , and SbP_3 is possible.^{3,13–15} Specifically in the case where $\text{E} = \text{As}$, treatment of $[\text{Na}][\text{P}_3\text{Nb}(\text{ODipp})_3]$ ($\text{Dipp} = 2,6$ -diisopropylphenyl) with 1 equiv of AsCl_3 affords AsP_3 in greater than 70% isolated yield as shown in Scheme 1, *i*.³ This reaction provides the first solution-phase synthesis of an interpnictide $\text{As}_n\text{P}_{4-n}$ ($n = 1–3$) tetrahedron.

Transition-metal chalcogenide chemistry provides us with a family of reactions bearing close relation to our synthesis of AsP_3 . Namely, treatment of Y_2X_2 ($\text{Y} = \text{S}, \text{Se}, \text{Te}$; $\text{X} = \text{Cl}$ or Br) with S_5TiCp_2 results in formation of Y_2S_5 and X_2TiCp_2 .^{16–18} The first example of such a reaction ($\text{Y} = \text{S}, \text{X} = \text{Cl}$) comes from a 1968 report by Schmidt and co-workers (Scheme 1, *ii*).¹⁶ When $\text{Y} = \text{Se}$ or Te , this reaction is an illustrative example of the solution synthesis of a heteroatomic interchalcogenide using transfer of S_5^{2-} from an early transition metal center to an M_2^{2+}

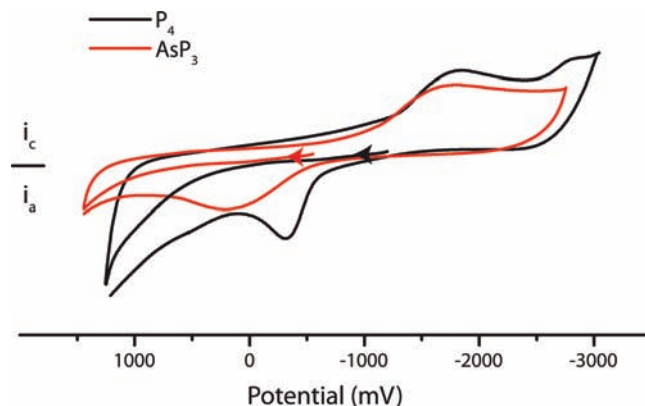


Figure 1. Cyclic voltammogram of P_4 (black) and AsP_3 (red). 0.25 M $[\text{NBu}_4][\text{PF}_6]$ in THF at 20 °C, sweep rate 300 mV s^{-1} , referenced vs Fc/Fc^+ , AsP_3 purified by sublimation (red), P_4 purified by recrystallization (black).

fragment. This is a close analogy to the solution synthesis of a heteroatomic interpnictide using transfer of P_3^{3-} from an early transition metal center to an As^{3+} fragment.

The physical properties of AsP_3 have been probed by a variety of methods. AsP_3 readily sublimates under vacuum at 60 °C and melts without decomposition at 72 °C.³ AsP_3 has been shown to be thermally stable in refluxing toluene solution for more than one week.³ Raman spectroscopy obtained on solid samples of AsP_3 shows four resonances at 313 (a_1), 345 (e), 428 (a_1), and 557 (e) cm^{-1} , consistent with calculated stretching modes for this C_{3v} symmetric molecule.³ High-resolution, electron-impact mass spectroscopy on a solid sample of AsP_3 has provided a mass of 167.8426 m/z .³ A solution molecular weight determination of AsP_3 gives a molecular weight of 167 ± 5 m/z (95% confidence level), confirming that the molecule also exists in the monomeric form when in solution. Finally, phosphorus NMR spectroscopy shows a single sharp resonance at -484 ppm in benzene solution.³ This shift is 36 ppm downfield of that for elemental phosphorus in the form of P_4 (discussed below).

Electronic Structure of AsP_3 . The electrochemical profiles of AsP_3 and P_4 have been compared using cyclic voltammetry in THF solution (Figure 1). P_4 has a single broad reduction event with onset at -1.3 V vs Fc/Fc^+ . This is the only observable reduction feature in the P_4 cyclic voltammogram (CV) and possibly indicates formation of the P_4 radical anion followed by irreversible bond rupture.¹⁹ Scanning cathodically, the CV of AsP_3 displays a similarly broad irreversible reduction event with onset at -1.0 V vs Fc/Fc^+ , which likely signifies more facile generation of AsP_3 radical anion and subsequent bond rupture. The earlier onset of reduction for AsP_3 suggests that the LUMO of AsP_3 is lower in energy than the LUMO of P_4 by approximately 10 kcal mol^{-1} . The calculated molecular orbitals for P_4 and AsP_3 show that the LUMO of AsP_3 is lower in energy by 4.9 kcal mol^{-1} (Figure 2). Scanning anodically from the rest potential, no observable oxidation events are initially observable in the solvent window of the experiment. Upon reduction however, both the AsP_3 and P_4 solutions show a single oxidation wave. Repeated scanning causes the oxidation

(12) Advisories to the Public. Red phosphorus, white phosphorus, and hypophosphorous acid are being used to make methamphetamine; Drug Enforcement Agency, Office of Diversion Control: Washington, DC, http://www.deadiversion.usdoj.gov/chem_prog/advisories/phosphorous.htm, June 18, 2009.

(13) Piro, N. A.; Cummins, C. C. *J. Am. Chem. Soc.* **2008**, *130*, 9524–9535.

(14) Piro, N. A.; Cummins, C. C. *Angew. Chem., Int. Ed.* **2009**, *48*, 934–938.

(15) Piro, N. A. Niobium-Mediated Generation of P-P Multiply Bonded Intermediates. Ph.D. Thesis; Massachusetts Institute of Technology: Cambridge, MA, June 2009.

(16) Schmidt, M.; Block, B.; Block, H. D.; Kopf, H.; Wilhelm, E. *Angew. Chem., Int. Ed. Engl.* **1968**, *7*, 632–633.

(17) Stuedel, R.; Papavassiliou, M.; Strauss, E.; Laitinen, R. *Angew. Chem., Int. Ed. Engl.* **1986**, *25*, 99–101.

(18) Stuedel, R.; Jensen, D.; Baumgart, F. *Polyhedron* **1990**, *9*, 1199–1208.

(19) The electrochemistry data were collected in 0.25 M $[\text{TBA}][\text{PF}_6]$ at a scan rate of 300 mV s^{-1} . A 1 mm diameter Pt disk working electrode, curly Pt wire counter electrode, and Ag wire pseudo-reference electrode were used for all measurements. All measurements were corrected to $\text{Cp}_2\text{Fe}^{0/+}$ by the addition of Cp_2Fe as an internal standard.

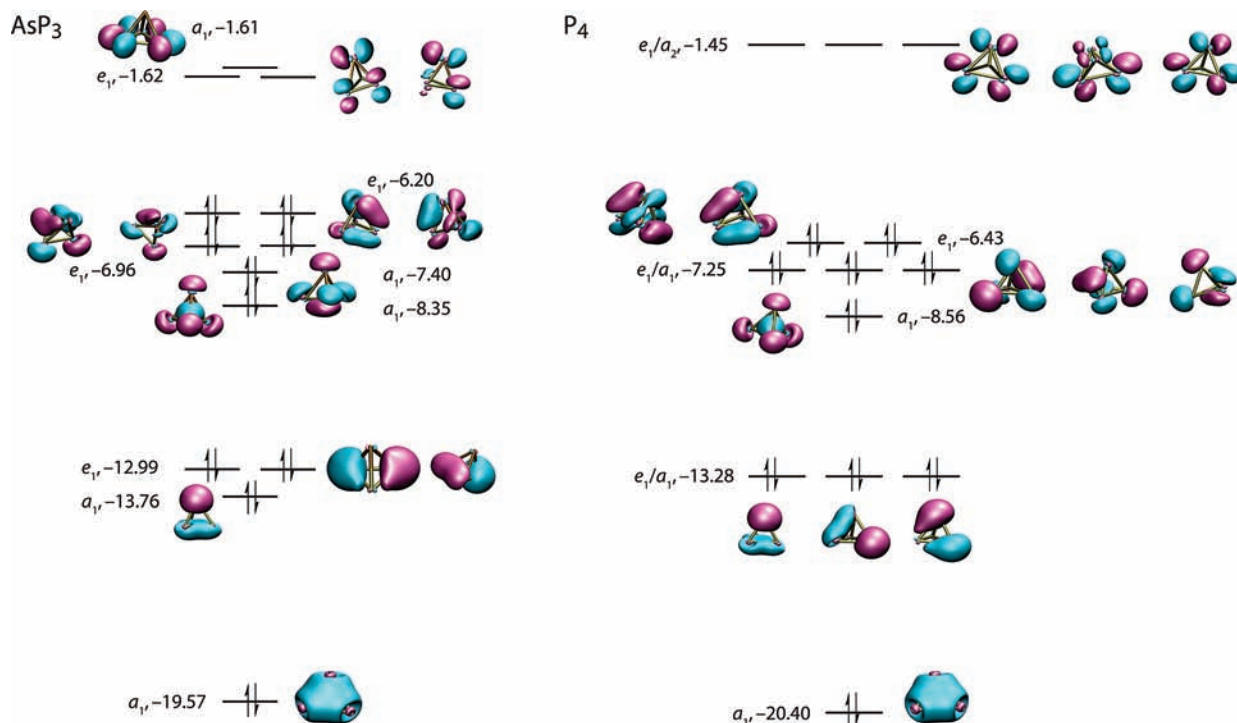


Figure 2. Molecular orbital diagrams for AsP₃ (left) and P₄ (right). Both diagrams were calculated using C_{3v} symmetry to allow for direct comparison of the calculated orbitals.

Table 1. NMR Shielding Tensors for AsP₃ and P₄

	σ_{dia}	σ_{para}	σ_{SO}	HLG (eV)
AsP ₃	954.694	-151.744	17.372	4.58
P ₄	953.301	-111.418	16.116	4.98

events to grow in intensity and shift slightly in potential, suggesting that they are a result of electropolymerization or some other complicating process. The observed stabilization of the AsP₃ LUMO renders reduction chemistry more facile and is certainly a contributor to the enhanced reactivity of AsP₃ as compared to P₄.

Closer scrutiny of the molecular orbital diagrams of AsP₃ and P₄ gives additional insight into the differences of these two related molecules (Figure 2). We find that the HOMO–LUMO energy gap of AsP₃ is smaller in magnitude by 0.40 eV as compared to that for P₄ (Figure 2). The lower-energy HOMO–LUMO gap of AsP₃ is manifest experimentally in the ³¹P NMR spectrum. It might be expected, on the basis of the electron density distribution in AsP₃, that the presence of the more electropositive As atom would increase the electron density at the phosphorus nuclei, causing the remaining three phosphorus atoms to be more shielded and resonate at higher field relative to P₄. This, however, is not the case. In benzene solution, P₄ resonates at -520 ppm in the ³¹P NMR spectrum, while the phosphorus atoms of AsP₃ resonate at -484 ppm. A decomposition of the NMR shielding terms, as calculated with ADF,^{20,21} reveals that the paramagnetic shielding term is the dominant contributor to the chemical shift (Table 1). The paramagnetic shielding term of AsP₃ is more negative by

approximately 40 ppm. This decrease in the paramagnetic term arises from greater coupling of the virtual and occupied orbitals due to the decrease in the HOMO–LUMO gap (HLG).²² Thus, it is the HLG, not the electron density at P, that is responsible for the observed chemical shift difference between P₄ and AsP₃.

An additional electronic property of note for comparison between P₄ and AsP₃ is the degree of spherical aromaticity harbored by these clusters.²³ Hirsch and co-workers have previously applied the concept of spherical aromaticity to a variety of T_d cage molecules including P₄ by calculating the nucleus-independent chemical shift (NICS) at the cage critical point.^{23,24} The NICS value for P₄ is known by this method to be large and negative, indicative of spherical aromaticity and large diamagnetic ring currents in the cluster. Following location of the cage critical points in P₄ and AsP₃, we find that the NICS value calculated for P₄, -59.444, is only one unit more negative than that found for AsP₃, -58.230. This indicates that despite the lowering in molecular symmetry upon going from P₄ to AsP₃, a great deal of spherical aromaticity is retained. The retention of spherical aromaticity is partially due to the fact that AsP₃, like P₄, maintains closed shell σ and π subsystems, resulting in symmetrically distributed angular momenta (Figure 2).²⁴

That the degree of spherical aromaticity in AsP₃ is not diminished relative to that of P₄ implies that the presence of the single As atom does not greatly perturb the charge distribution. There are two limiting views of the charge distribution in AsP₃: one view is that AsP₃ contains an As³⁺ ion supported by a P₃³⁻ unit, while an alternative view is that

(20) te Velde, G.; Bickelhaupt, F. M.; Baerends, E. J.; Fonseca Guerra, C.; van Gisbergen, S. J. A.; Snijders, J. G.; Ziegler, T. J. *J. Comput. Chem.* **2001**, *22*, 931–967.
 (21) Fonseca Guerra, C.; Snijders, J. G.; te Velde, G.; Baerends, E. J. *Theor. Chem. Acc.* **1998**, *99*, 391–403.

(22) Widdifield, C. M.; Schurko, R. W. *Concept. Magn. Reson. A* **2009**, *34A*, 91–123.
 (23) Schleyer, P. V.; Maerker, C.; Dransfeld, A.; Jiao, H.; Hommes, N. *J. Am. Chem. Soc.* **1996**, *118*, 6317–6318.
 (24) Hirsch, A.; Chen, Z.; Jiao, H. *Angew. Chem., Int. Ed.* **2001**, *40*, 2834–2838.

Table 2. Calculated Atomic Charges for AsP₃

	AIM (<i>e</i>)	Hirshfeld (<i>e</i>)	Voronoi (<i>e</i>)
As	+0.126	+0.0461	+0.051
P	-0.042	-0.015	-0.018

Table 3. Heats of Atomization, Bond Energies, and Standard Heats of Formation for As_{*n*}P_{4-*n*}

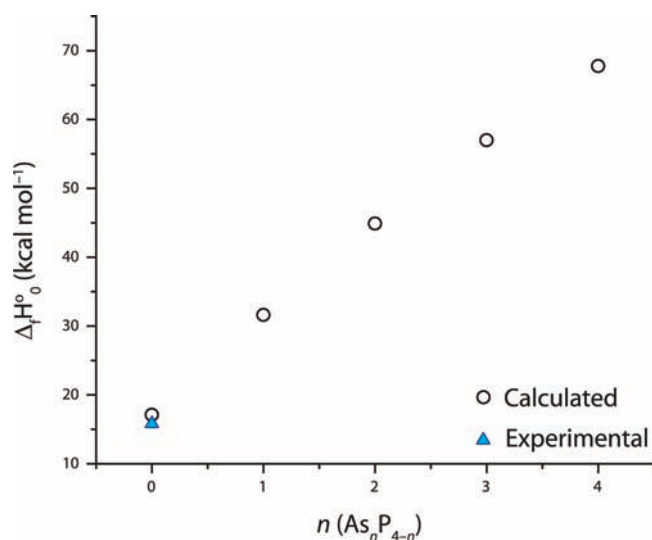
	heat of atomization calculated ^a kcal mol ⁻¹	bond energy calculated ^b kcal mol ⁻¹	Δ _f H ^o calculated ^c kcal mol ⁻¹
P ₄	284	P–P 47	17
AsP ₃	266	P–P 47 As–P 41	32
As ₂ P ₂	250	P–P 47 As–P 41 As–As 36	45
As ₃ P	234	As–P 41 As–As 36	57
As ₄	220	As–As 36	68

^a Heat of atomization = |total bonding energy As_{*n*}P_{4-*n*} – |(*n* (energy ⁴S As atoms) + (4-*n* (energy ⁴S P atom)) | – |zero-point energy|. ^b Heat of atomization/6. ^c Δ_fH^o = Σ(Δ_fH^o constituent atoms)³² – heat of atomization.

AsP₃ contains neutral P atoms and a neutral As atom. Calculations using the AIM method have suggested that the phosphorus atoms of AsP₃ harbor a very slight negative charge of -0.04 *e* and the arsenic atom makes up the balance, having a slight positive charge of +0.12 *e*. Table 2 compiles the charge descriptions given by the AIM method, as well as the Hirshfeld and Voroni Deformation Density methods.^{25,26} All three methods give generally good agreement of the assigned charges and support the description that AsP₃ contains a neutral As atom and three neutral P atoms. This charge distribution informs our description of AsP₃ as a soluble, molecular combination of these two elements. This analysis is in agreement with more simple interpretations based on Pauling electronegativities (P, 2.19 and As, 2.18), as well as with more complicated theoretical descriptions (Figure 1S, Supporting Information).^{27,28}

In order to obtain a more quantitative depiction of the As–P and P–P bond energies in AsP₃, we investigated the heats of atomization of AsP₃, As₂P₂, As₃P, P₄, and As₄, in order to calculate average bond energies for these species.²⁷ Heats of atomization are computed as an energy difference between the molecule and the single atoms. The individual atoms are computed as spherically symmetric and spin-restricted.²⁹ In order to accurately represent the true atomic ground state, we calculated the fragment energy of a single P atom with three α spins (⁴S ground state).²⁹ After correction for the true atomic ground state and for the zero-point energy of the molecule, we obtained reliable and accurate heats of atomization as shown in Table 3.²⁸ These data permit estimation of the bond dissociation energies; for example, the P₄ molecule is composed of six P–P bonds, so division of the heat of atomization of P₄ by six gives an estimate of the P–P bond energy.²⁷ Our calculations put the P–P bond energy of P₄ at 47 kcal mol⁻¹, which compares perfectly with the 47 kcal mol⁻¹ obtained from

- (25) Nalewajski, R. F. *Phys. Chem. Chem. Phys.* **2002**, *4*, 1710–1721.
 (26) Fonseca Guerra, C.; Handgraaf, J. W.; Baerends, E. J.; Bickelhaupt, F. M. *J. Comput. Chem.* **2003**, *25*, 189.
 (27) Pauling, L. *The Nature of the Chemical Bond*, 3rd ed.; Cornell University Press: Ithaca, 1960.
 (28) Please see the Supporting Information for further details.
 (29) Baerends, E. J.; Branchadell, V.; Sodupe, M. *Chem. Phys. Lett.* **1997**, *265*, 481–489.

**Figure 3.** Plot of Δ_fH^o vs *n* for As_{*n*}P_{4-*n*}.

experimental values.³⁰ Using this energy for the P–P bonds, we can extend our method to AsP₃. Following subtraction of 3 P–P single bond energies from the heat of atomization we computed for AsP₃, we are left with 3 As–P bonds; with an estimated bond dissociation energy of 41 kcal mol⁻¹ each. Similarly, the As–As bonds of As₄ were found to have bond dissociation energies of 36 kcal mol⁻¹. Keeping the P–P and As–As bond energies constant, extraction of P–As bond energies from the heats of atomization of As₂P₂ and As₃P give the same value of 41 kcal mol⁻¹ (Table 3). In summary, our calculations indicate that the As–P bonds of AsP₃ are 6 kcal mol⁻¹ weaker than the P–P bonds of P₄ (and 5 kcal mol⁻¹ stronger than the As–As bonds of As₄). This is in agreement with our observations of the enhanced reactivity of these bonds (*vide infra*) relative to P₄ as well as reported values for typical P–P, P–As, and As–As single bond strengths.³¹

From the calculated values for heats of atomization and the known heats of formation of the As and P atoms at 0 K, we are able to extract estimated heats of formation at 0 K for As_{*n*}P_{4-*n*} by summation of the experimental heats of formation of the constituent atoms followed by subtraction of the calculated heats of atomization (Table 3). As would be expected, there is a monotonic increase in the standard heats of formation with increasing *n* (Table 3, Figure 3). This trend in heats of formation begins to shed light on the thermodynamic stability of these tetrahedral pnictogen molecules and shows that upon increasing the arsenic content there is a significant price to pay for formation of As_{*n*}P_{4-*n*} from the elements in their standard states.

Reactivity Studies. A series of reactivity studies has been carried out with AsP₃. The reactions chosen have previously been successfully carried out with P₄ and include thermolysis, adduct formation, single bond cleavage reactions by transition metal and organic radicals, and molecule activation with Nb(H)(η²-Bu(H)C=NAr)(N[CH₂Bu]Ar)₂ (Ar = 3,5-Me₂C₆H₃), Mo(N[^tBu]Ar)₃, and Cl₂Nb(ODipp)₃ under reducing conditions. In looking at such a class of reactions we hope to compare the

- (30) Tsirelson, V. G.; Tarasova, N. P.; Bobrov, M. F.; Smetannikov, Y. V. *Heteroatom. Chem.* **2006**, *17*, 572–578.
 (31) Norman, N. C. *Chemistry of Arsenic, Antimony, and Bismuth*; Springer: New York, 1998.
 (32) Chase, M. W. *NIST-JANAF Thermochemical Tables*; American Institute of Physics: Melville, NY (*J. Phys. Chem. Ref. Data*, Monograph 9), 1988; Vol. 28, Iss. 6.

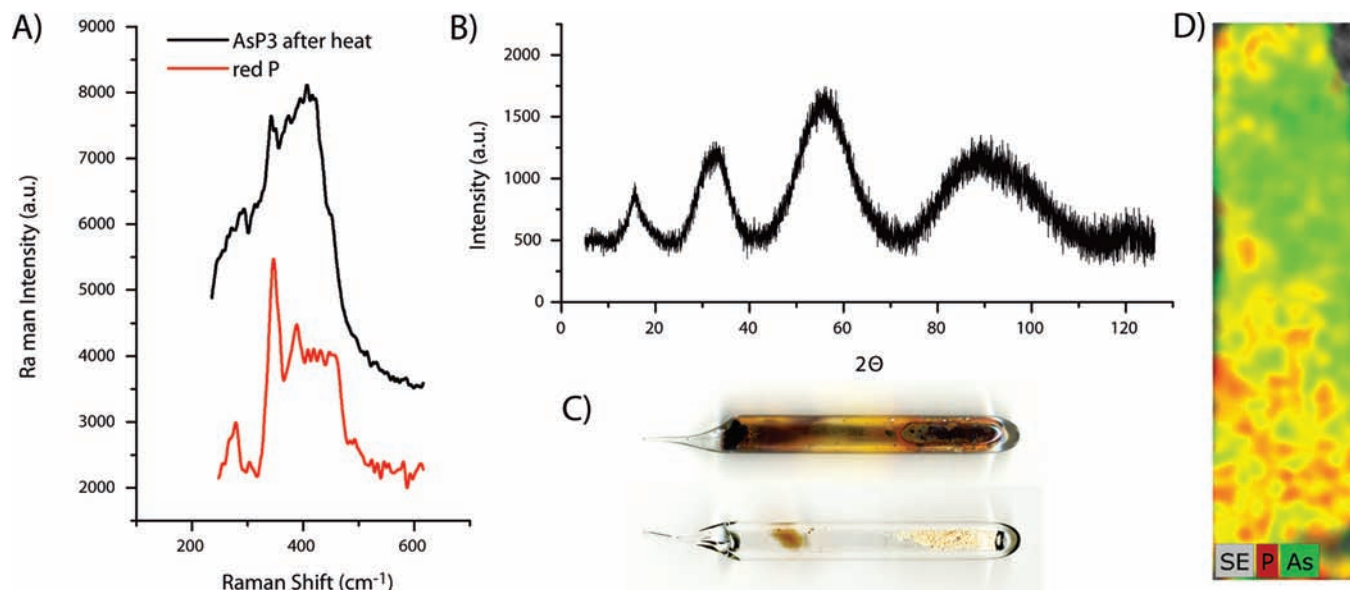


Figure 4. Thermal decomposition of AsP₃ to metallic arsenic and red phosphorus. (A) Raman spectra of the product of heating AsP₃ (black) and an authentic sample of red phosphorus (red). (B) Powder XRD data for the product of heating AsP₃. (C) Photographs of the reaction vessel before heating (bottom) and after heating (top). (D) Elemental mapping by EDS analysis using an SEM microscope.

reactivity patterns of P₄ and AsP₃ in light of their contrasting physical and electronic properties as elucidated in the theoretical studies.

Thermolysis of AsP₃. Amorphous red phosphorus was first obtained in 1848 by heating P₄ in the absence of air for several days at high temperatures, and is now made on a commercial scale of 7000 tons per year by a similar thermal conversion process.² Red phosphorus is much less toxic and much less reactive than monomeric white phosphorus and it is extensively used in the production of matches, flame retardants, and phosphide materials for semiconductor applications.² Semiconductor applications account for a majority of red phosphorus consumption, with aluminum phosphide production accounting for over 24% of the total consumption. Much of this aluminum phosphide is further alloyed with species such as gallium arsenide to tune the semiconductor band gap.^{1,2}

Polymeric forms of P/As alloys are exceedingly rare.^{33,34} Intrigued by the possibility of a “red AsP₃” phase wherein one out of every four sites in red P would be occupied by an As atom, we subjected AsP₃ to the same conditions under which P₄ converts to red P. Heating a sealed tube containing white AsP₃ to 300 °C for 36 h resulted in apparent segregation of the elements, producing amorphous metallic arsenic and amorphous red phosphorus, as determined by Raman spectroscopy (diagnostic for red P³⁵), powder XRD analysis (diagnostic for amorphous metallic As³⁶), and EDS elemental analysis of the bulk material (Figure 4). The EDS elemental map shown in Figure 4 shows distinct regions where only phosphorus (red) and only arsenic (green) are sequestered; however, there are some regions (yellow) where the two species may be found together, suggestive of incomplete separation. Repetition of this experiment on a variety of scales gave reproducible results.

Thermal decomposition of AsP₃ to the elements is quite surprising and the mechanism by which this occurs is not known. One possibility is that under thermal conditions four molecules of AsP₃ disproportionate to give rise to three molecules P₄ and one molecule of As₄, which themselves then revert to red phosphorus and metallic arsenic. From our calculated heats of formation (Figure 2), we can get an estimate for the heat of disproportionation of four molecules of AsP₃ to give three molecules of P₄ and one molecule of As₄. In so doing we find that the process is downhill by 7.42 kcal mol, suggesting that the kinetic stability of AsP₃ is quite important in its isolability, as thermodynamically it is only metastable. An alternative mechanism might involve the formation of “red AsP₃”, which is not itself thermally robust, reverting to red phosphorus and metallic arsenic. It may be speculated that an alternative to the thermal pathway may yet be successful in leading to a red polymeric form of AsP₃, and preliminary studies on AsP₃ polymerization by radical initiators and UV light are under way.

Coordination Chemistry of AsP₃. In our initial report on the facile synthesis of AsP₃ we used the complex (μ-N₂)[Mo(CO)₃-(PⁱPr₃)₂]₂ to complex the AsP₃ tetrahedron and to provide a structural glimpse of the intact tetrahedron (Scheme 2, *i*).³ Unfortunately, the AsP₃ adduct, (AsP₃)Mo(CO)₃(PⁱPr₃)₂ was unstable above 0 °C and for that reason was difficult to work with. Additionally, accurate determination of the As–P interatomic distances in (AsP₃)Mo(CO)₃(PⁱPr₃)₂ was hampered by a 70:30 disorder between the As atom and one of the two noncomplexed P atoms in the tetrahedron. Thus, we sought to synthesize a more thermally stable adduct of AsP₃ and hoped to obtain accurate metrical parameters from an ordered crystal structure.

The precursor FeCp*(dppe)Cl, which had been reported to form a stable P₄ adduct,³⁷ has allowed us to realize this goal. Treatment of dark-green FeCp*(dppe)Cl with 1 equiv of AsP₃

(33) Jayasekera, B.; Somaskandan, K.; Brock, S. L. *Inorg. Chem.* **2004**, *43*, 6902–6904.

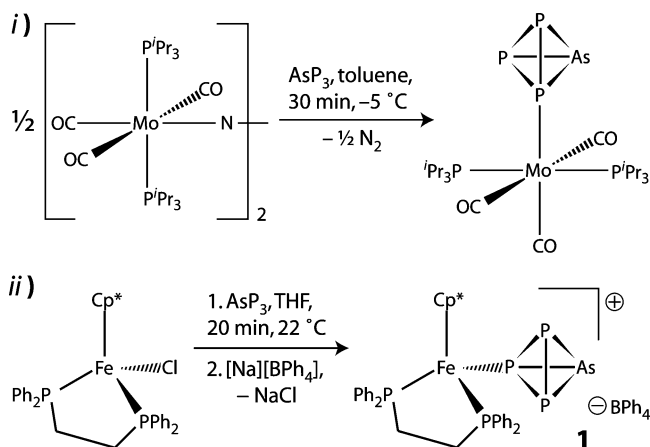
(34) Von Schnering, H. G.; Honle, W. *Chem. Rev.* **1988**, *88*, 243–273.

(35) Fasol, G.; Cardona, M.; Honle, W.; Von Schnering, H. G. *Solid State Commun.* **1984**, *52*, 307–310.

(36) Breitling, G. *Mater. Res. Bull.* **1969**, *4*, 19–32.

(37) de los Rios, I.; Hamon, J. R.; Hamon, P.; Lapinte, C.; Toupet, L.; Romerosa, A.; Peruzzini, M. *Angew. Chem., Int. Ed.* **2001**, *40*, 3910–3912.

Scheme 2



in THF results in a gradual color change to brown over 20 min. Subsequent treatment of the reaction mixture with 1 equiv of NaBPh₄ results in an immediate color change to bright magenta. Following removal of the NaCl byproduct, [(AsP₃)Fe-Cp*(dppe)][BPh₄], **1**, was isolated in 80% yield by recrystallization of the crude solids from 1:1 Et₂O/THF (Scheme 2, *ii*). X-ray diffraction quality crystals of **1** were grown from a mixture of THF and CH₂Cl₂ at -35 °C over the course of several days. The X-ray structure of **1** (Figure 5) displays a fully ordered AsP₃ tetrahedron in an η¹ binding mode at a phosphorus vertex (Table 1S, Supporting Information). The solid-state structure of **1** is consistent with the solution-state configuration of the AsP₃ unit as assigned by NMR spectroscopy (Supporting Information Figure 2S). The P12–As1 and P12–P13,14 distances in **1** are 2.283(2) Å and 2.183(3) Å, respectively, and are noticeably shorter than typical P–As and P–P single bonds. The other As–P and P–P bonds are noticeably longer with As1–P13 at 2.334(2) Å, As1–P14 at 2.336(2) Å, and P13–P14 at 2.231(3) Å. The shortened bond lengths to P12 are the effect of rehybridization that occurs upon AsP₃ binding to the Fe center, producing greater 3s character in the bonding molecular orbitals of this four-coordinate phosphorus atom. It is noteworthy that the Fe1–P12 interatomic distance of 2.172(2) Å is significantly shorter than the Fe–phosphine bond distances at 2.233(2) Å and 2.242(2) Å.

As–P Bond Cleavage Reactions. The estimated 6 kcal mol⁻¹ difference in energy between the As–P bonds and the P–P bonds in AsP₃ suggests that reactions resulting in selective As–P bond cleavage may be possible. Several systems are known to promote radical opening of the P₄ tetrahedron to produce substituted tetraphosphabicyclobutane structures. A noteworthy example of this reaction type was reported by Lappert and co-workers and uses (P(N(ⁱPr)₂)N(SiMe₃)₂)₂ as a source of the phosphorus radical •P(N(ⁱPr)₂)N(SiMe₃)₂, which was shown to activate P₄ to produce the corresponding 1,4-bis(phosphido)tetraphosphabicyclobutane.³⁸ While activation of P₄ by (P(N(ⁱPr)₂)N(SiMe₃)₂)₂ requires somewhat harsh conditions (refluxing in toluene for 1.5 h), the corresponding reaction with AsP₃ is rapid at room temperature. Upon mixing (P(N(ⁱPr)₂)N(SiMe₃)₂)₂ with 1 equiv of AsP₃ in toluene the initially colorless reaction mixture turns bright yellow. NMR spectroscopic analysis of the crude reaction mixture shows clean and quantitative conversion to AsP₃(P(N(ⁱPr)₂)N(SiMe₃)₂)₂ (set of isomers), **2**, in which a

single As–P bond has been selectively cleaved, as assigned by ³¹P NMR spectroscopy (Scheme 3, *i*, and Figure 3S, Supporting Information). Recrystallization of the crude reaction mixture from *n*-hexane/Et₂O gave crystalline **2** in 88% yield. X-ray crystallographic analysis on a single crystal of **2** confirmed the selective As–P bond cleavage as shown in Figure 6 and Table 2S, Supporting Information. The geometrical parameters of the arsatriphosphabicyclobutane core of **2** are nearly isomorphous with the all-phosphorus analogue as reported by Lappert and co-workers.³⁸ A discussion of accurate P–P and As–P bond lengths is precluded by disorder in the crystal structure of **2**. Notably, there is a positional disorder of As1 and P1, but there is no As component to the P2 or P3 positions.

The bright green Ti(III) reagent Ti(N[^tBu]Ar)₃ (Ar = 3,5-Me₂C₆H₃) has proven to be a potent metalloradical and one-electron reductant since its first synthesis by reduction of the corresponding ClTi(N[^tBu]Ar)₃ complex in 1995.^{39–43} Given the facile radical opening of the AsP₃ tetrahedron with (P(N(ⁱPr)₂)N(SiMe₃)₂)₂, we hypothesized that Ti(N[^tBu]Ar)₃ would be a good candidate for forming a 1,4-bis(metallo)arsatriphosphabicyclobutane. In fact, Ti(N[^tBu]Ar)₃ does react with AsP₃ to generate the desired 1,4-bis(metallo)arsatriphosphabicyclobutane, AsP₃(Ti(N[^tBu]Ar)₃)₂, **3-AsP₃**, in which a single As–P bond has been cleaved selectively; however, the reaction does not go to completion. Instead, an equilibrium is established between AsP₃, Ti(N[^tBu]Ar)₃, and **3-AsP₃** (Scheme 3, *ii*). This equilibrium was studied by ³¹P NMR spectroscopy at a variety of concentrations and temperatures. In all cases the equilibrium favored the reactants, with **3-AsP₃** never accounting for more than 30% of the reaction mixture (Figures 4S, 14S, 15S, Supporting Information).⁴⁴ The analogous reaction with P₄ likewise gave an equilibrium mixture, but the 1,4-bis(metallo)tetraphosphabicyclobutane product, P₄(Ti(N[^tBu]Ar)₃)₂, **3-P₄**, never accounted for more than 5% of the reaction mixture under identical conditions. Although no intermediates were detected in these equilibria, the systems did not conform to the simple equilibrium expression, $K_{eq} = 3/[Ti(N[{}^tBu]Ar)_3]^2[EP_3]$ (E = As, P), suggesting that more complicated processes are at work. It should be noted that the concentration of Ti(N[^tBu]Ar)₃ was obtained by subtraction of 2[**3-E₄**] from [Ti(N[^tBu]Ar)₃]₀. In direct competition reactions, the tendency of Ti(N[^tBu]Ar)₃ to react with EP₃ (E = P, As) to form the radical-opened bicyclobutane derivatives, **3-AsP₃** and **3-P₄**, revealed a measurable preference for edge-opening of AsP₃, (Figures 14S and 15S, Supporting Information), consistent with heightened reactivity for AsP₃ over P₄ (*vide supra*). One hypothesis for why Ti(N[^tBu]Ar)₃ is unsuccessful at driving the radical cleavage of either P₄ or AsP₃ fully to **3-EP₃** (E = P, As) is centered upon the unfavorable loss in entropy inherent in forming a single-product molecule from three reactant molecules. The interaction

(38) Bezombes, J. P.; Hitchcock, P. B.; Lappert, M. F.; Nycz, J. E. *Dalton Trans.* **2004**, 499–501.

(39) Wanandi, P. W.; Davis, W. M.; Cummins, C. C. *J. Am. Chem. Soc.* **1995**, *117*, 2110–2111.

(40) Peters, J. C.; Johnson, A. R.; Odom, A. L.; Wanandi, P. W.; Davis, W. M.; Cummins, C. C. *J. Am. Chem. Soc.* **1996**, *118*, 10175–10188.

(41) Agapie, T.; Diaconescu, P. L.; Mendiola, D. J.; Cummins, C. C. *Organometallics* **2002**, *21*, 1329–1340.

(42) Agarwal, P.; Piro, N. A.; Meyer, K.; Muller, P.; Cummins, C. C. *Angew. Chem., Int. Ed.* **2007**, *46*, 3111–3114.

(43) Kim, E.; Odom, A. L.; Cummins, C. C. *Inorg. Chim. Acta* **1998**, *278*, 103–107.

(44) Concentrations of AsP₃ and **3-AsP₃** were determined by integration against an internal standard (PPh₃). The concentration of Ti(N[^tBu]Ar)₃ was inferred using the equation [Ti(N[^tBu]Ar)₃]_f = [Ti(N[^tBu]Ar)₃]₀ – 2[**3-AsP₃**]_f. This assumes no other degradation pathways are operative during the course of the reaction.

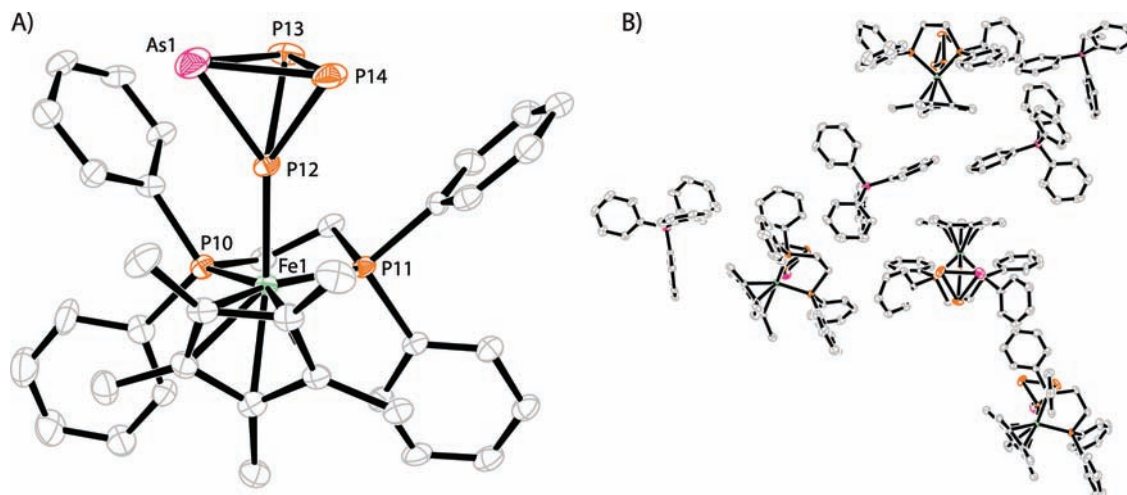
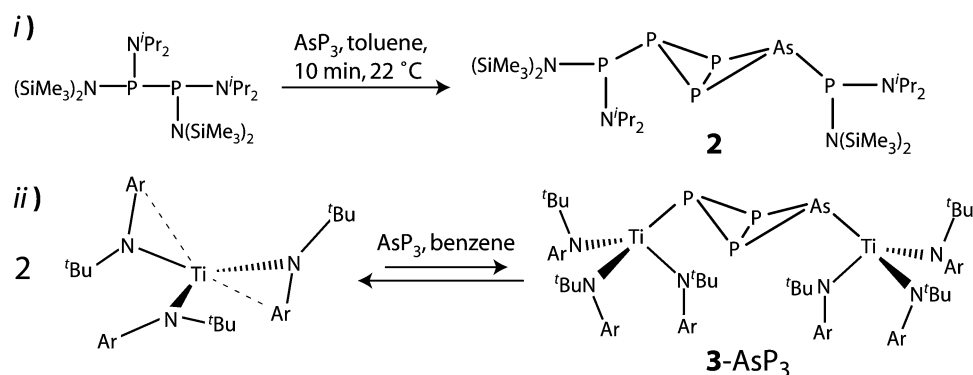


Figure 5. Solid-state structure of complex **1** shown with 50% probability thermal ellipsoids. (A) View of the $[(\text{AsP}_3)\text{FeCp}^*(\text{dppe})]^+$ core. (B) View of the asymmetric unit. Hydrogen atoms and CH_2Cl_2 solvent residues have been omitted for clarity.

Scheme 3



between the hard titanium(IV) metal center and the soft phosphorus (or arsenic) center does not provide a large enough enthalpic contribution to counterbalance the entropic losses incurred.

Formation of $\mu_2:\eta^2,\eta^2\text{-E}_2\text{Nb}_2$ Complexes (E = As, P). The activation of white phosphorus by early transition-metal complexes has been a prolific area of investigation in recent years.^{45–48} Included among these are niobium complexes bearing three monoanionic ligands. This class of complexes has given rise to a wide array of P_n ligands ($n = 1–8$).^{3,45,49,50}

The metallaziridine(hydride) derivative, $\text{Nb}(\text{H})(\eta^2\text{-}^t\text{Bu}(\text{H})\text{C}=\text{NAr})(\text{N}[\text{CH}_2^t\text{Bu}]\text{Ar})_2$ (Ar = 3,5-Me₂C₆H₃), was found to react with 0.25 equiv of white phosphorus to quantitatively give rise to the corresponding $(\mu_2:\eta^2,\eta^2\text{-P}_2)[\text{Nb}(\text{N}[\text{CH}_2^t\text{Bu}]\text{Ar})_3]_2$ complex, which has a diagnostic phosphorus NMR resonance at 399 ppm in C₆D₆. Because of the high efficiency of this reaction it seemed to be an ideal candidate for reactivity tests with AsP_3 , with an eye toward formation of $(\mu_2:\eta^2,\eta^2\text{-P}_2)[\text{Nb}(\text{N}[\text{CH}_2^t\text{Bu}]\text{Ar})_3]_2$ and $(\mu_2:\eta^2,\eta^2\text{-AsP})[\text{Nb}(\text{N}[\text{CH}_2^t\text{Bu}]\text{Ar})_3]_2$ in a 1:1 ratio. In fact, treatment of bright yellow $\text{Nb}(\text{H})(\eta^2\text{-}^t\text{Bu}(\text{H})\text{C}=\text{NAr})(\text{N}[\text{CH}_2\text{-}$

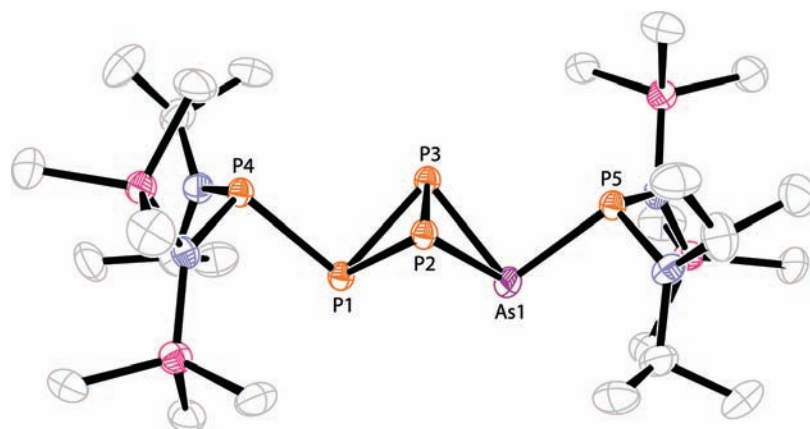
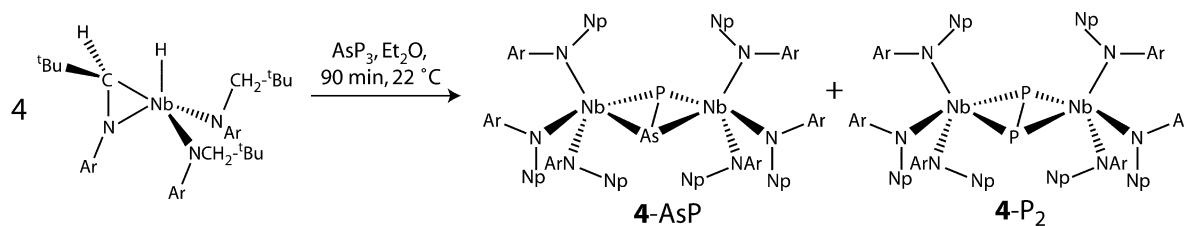
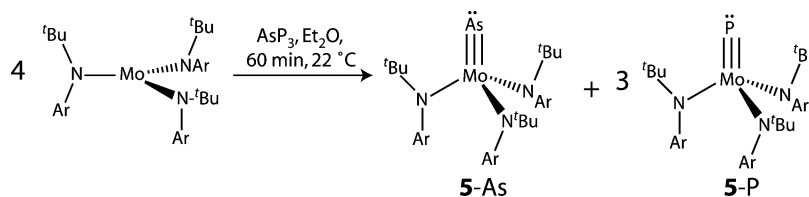


Figure 6. Solid-state structure of compound **2** with 50% probability thermal ellipsoids. Hydrogen atoms are omitted for clarity.

Scheme 4



Scheme 5



$^t\text{Bu}[\text{Ar}]_2$ with a slight excess (0.35 equiv) of AsP_3 results in clean and complete conversion to the expected 1:1 green mixture of products, $(\mu_2:\eta^2,\eta^2\text{-P}_2)[\text{Nb}(\text{N}[\text{CH}_2^t\text{Bu}]\text{Ar})_3]_2$, **4-P₂**, and $(\mu_2:\eta^2,\eta^2\text{-AsP})[\text{Nb}(\text{N}[\text{CH}_2^t\text{Bu}]\text{Ar})_3]_2$, **4-AsP**, over the course of 90 min (Scheme 4). ^{31}P NMR spectroscopic analysis of the crude reaction mixture shows exclusively two resonances in a 2:1 ratio at 399 and 438 ppm, respectively (Figure 5S, Supporting Information). Assignment of the resonance at 438 ppm to **4-AsP** was corroborated by DFT NMR shielding calculations.²⁸ This reaction provides access to a rare AsP ligand bridging two niobium metal centers, and future work with **4-AsP** will be aimed at identifying reactions in which the AsP unit is released.^{51–53}

Formation of Terminal E≡M Complexes (E = As, P). P_4 degradation to P_1 units has been observed in the treatment of the reactive Mo(III) precursor $\text{Mo}(\text{N}[\text{Bu}]\text{Ar})_3$ with 0.25 equiv of P_4 to give the $\text{P}\equiv\text{Mo}(\text{N}[\text{Bu}]\text{Ar})_3$ complex.⁵⁴ Access to the arsenide congener of $\text{P}\equiv\text{Mo}(\text{N}[\text{Bu}]\text{Ar})_3$ is also afforded by the corresponding reaction with As_4 ; however, this experiment is challenging as As_4 is unisolable.⁵⁵ A soluble, isolable source of As^0 would be preferable to obtain a stoichiometric transformation to the terminal arsenide complex, and AsP_3 proves to be an effective source of a single As^0 equivalent. Treatment of $\text{Mo}(\text{N}[\text{Bu}]\text{Ar})_3$ with a slight excess of AsP_3 (0.29 equiv) results in formation of a 1:3 mixture of $\text{As}\equiv\text{Mo}(\text{N}[\text{Bu}]\text{Ar})_3$, **5-As**, and $\text{P}\equiv\text{Mo}(\text{N}[\text{Bu}]\text{Ar})_3$, **5-P**, over the course of 1 h (Scheme 5). The ^1H NMR spectroscopic features for **5-As** and **5-P** are coincident,

but the corresponding ^{13}C NMR spectroscopic features are distinct and reveal that the reaction cleanly forms **5-As** and **5-P** in a 1:3 ratio (Figure 6S, Supporting Information). Interestingly, it was found that in 1:1 competition experiments of AsP_3 and P_4 with $\text{Mo}(\text{N}[\text{Bu}]\text{Ar})_3$, there is no selectivity for reaction with AsP_3 over P_4 (Figure 16S, Supporting Information). This is a striking example of a reaction in which AsP_3 does not give enhanced reactivity over P_4 , and is an interesting case. The reaction of AsP_3 with $\text{Mo}(\text{N}[\text{Bu}]\text{Ar})_3$ gives us clear proof that AsP_3 functions experimentally as a soluble source of As^0 and P^0 and also provides motivation for future studies in the synthesis of precise 3:1 mixtures of metal phosphides and metal arsenides for materials applications.^{56–58}

Formation of *cyclo*-E₃ Complexes (E = As, P), As_2P_2 , and As_2P . Our original synthesis of AsP_3 involved treatment of an anionic niobium *cyclo*- P_3 complex with AsCl_3 to obtain the tetraatomic tetrahedron. Since that discovery, we have been interested in preparing other anionic *cyclo*-E₃ compounds, in particular an anionic *cyclo*- As_2P complex. Such a species could, in principle, be used to synthesize the previously unexplored tetraatomic interpnictides As_2P_2 and As_3P by treatment of the *cyclo*- As_2P derivative with the appropriate ECl_3 reagent (E = P, As). Strides in this direction have been made by investigating the reaction between AsP_3 and $\text{Cl}_2\text{Nb}(\text{ODipp})_3$ in the presence of a reducing agent.^{3,59} Combining AsP_3 with $\text{Cl}_2\text{Nb}(\text{ODipp})_3$ in a 1:1 ratio in THF followed by treatment with Na/Hg amalgam gives rise to a mixture of $[\text{Na}][\text{P}_3\text{Nb}(\text{ODipp})_3]$, **6-P₃**, $[\text{Na}][\text{As}_2\text{P}_2\text{Nb}(\text{ODipp})_3]$, **6-AsP₂**, $[\text{Na}][\text{As}_2\text{PNb}(\text{ODipp})_3]$, **6-As₂P**, and presumably, $[\text{Na}][\text{As}_3\text{Nb}(\text{ODipp})_3]$, **6-As₃**, over the course of 30 min. Evidence for formation of **6-P₃**, **6-AsP₂**, and **6-As₂P** in a 10:5:1 molar ratio (76% yield from $\text{Cl}_2\text{Nb}(\text{ODipp})_3$) is provided by the clean appearance of three singlets in the ^{31}P NMR spectrum of the crude reaction mixture, spaced as expected for sequential As-doping of the *cyclo*- P_3 complex (*vide supra*) at -206 (**6-P₃**), -167 (**6-AsP₂**), and -132 ppm (**6-As₂P**) (Figure 7S, Supporting Information). From the considerable

- (45) Figueroa, J. S.; Cummins, C. C. *Dalton Trans.* **2006**, 2161–2168.
 (46) Ehse, M. P.; Romerosa, A.; Peruzzini, M. *Top. Curr. Chem.* **2002**, *220*, 107–140.
 (47) Peruzzini, M.; Gonsalvi, L.; Romerosa, A. *Chem. Soc. Rev.* **2005**, *34*, 1038–1047.
 (48) Scherer, O. J. *Acc. Chem. Res.* **1999**, *32*, 751–762.
 (49) Cossairt, B. M.; Cummins, C. C. *Angew. Chem., Int. Ed.* **2008**, *47*, 169–172.
 (50) Piro, N. A.; Figueroa, J. S.; McKellar, J. T.; Cummins, C. C. *Science* **2006**, *313*, 1276–1279.
 (51) Umbarkar, S.; Sekar, P.; Scheer, M. J. *Chem. Soc. Dalton Trans.* **2000**, 1135–1137.
 (52) Davies, J. E.; Mays, M. J.; Raithby, P. R.; Shields, G. P.; Tompkin, P. K.; Woods, A. D. *J. Chem. Soc. Dalton Trans.* **2000**, 1925–1930.
 (53) Davies, J. E.; Kerr, L. C.; Mays, M. J.; Raithby, P. R.; Tompkin, P. K.; Woods, A. D. *Angew. Chem., Int. Ed.* **1998**, *37*, 1428–1429.
 (54) Laplaza, C. E.; Davis, W. M.; Cummins, C. C. *Angew. Chem., Int. Ed. Engl.* **1995**, *34*, 2042–2044.
 (55) Curley, J. C.; Piro, N. A.; Cummins, C. C. *Inorg. Chem.* **2009**, *48*, 10121–10126.

- (56) Carencio, S.; Resa, I.; LeGoff, X.; LeFloch, P.; Mezailles, N. *Chem. Commun.* **2008**, 2568–2570.
 (57) Yan, P.; Xie, Y.; Wang, W.; Liu, F.; Qian, Y. *J. Mater. Chem.* **1999**, *9*, 1831–1833.
 (58) Li, B.; Xie, Y.; Jiaying, H.; Liu, Y.; Qian, Y. *Ultrason. Sonochem.* **2001**, *8*, 331–334.
 (59) Clark, J. R.; Pulvirenti, A. L.; Fanwick, P. E.; Sigalas, M.; Eisenstein, O.; Rothwell, I. P. *Inorg. Chem.* **1997**, *36*, 3623–3631.

Scheme 6

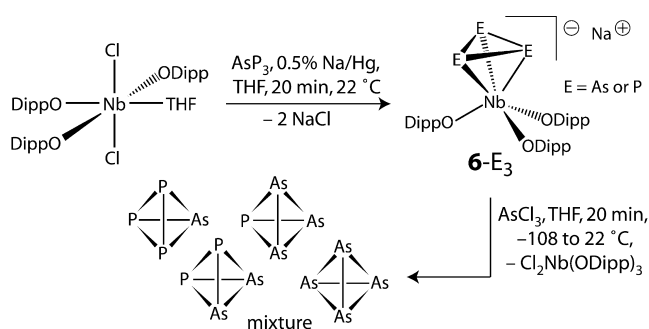


Table 4. NMR and GC–MS Data for Syntheses of AsP₃, As₂P₂, As₃P, and As₄

	P ₄ (internal standard)	AsP ₃	As ₂ P ₂	As ₃ P	As ₄
³¹ P shift (ppm)	–520	–484	–452	–432	N/A
calculated ³¹ P shift (ppm)	–520	–482	–451	–424	N/A
GC–MS retention time ^a	7.8 min	8.9 min	9.8 min	10.6 min	11.2 min
GC–MS mass (<i>m/z</i>)	124	168	212	256	300
GC–MS area (au)	50994	30475	11348	3176	~1977
yield ^b	N/A	49% ^c	39% ^d	50% ^e	2% ^f

^a GC–MS data were collected using an Agilent 6890N network GC system with an Agilent 5973 Network mass selective detector and an Rtx-1 column from Restek. ^b Yields of AsP₃, As₂P₂, and As₃P are calculated from the corresponding starting concentration of 6-E₃; in each case the theoretical yield is 100%; for As₄ the yield is calculated from the starting concentration of Cl₂Nb(ODipp)₃ making the theoretical yield ≪100%. ^c GC–MS yield from 6-P₃. ^d GC–MS yield from 6-AsP₂. ^e GC–MS yield from 6-As₂P. ^f GC–MS yield from Cl₂Nb(ODipp)₃.

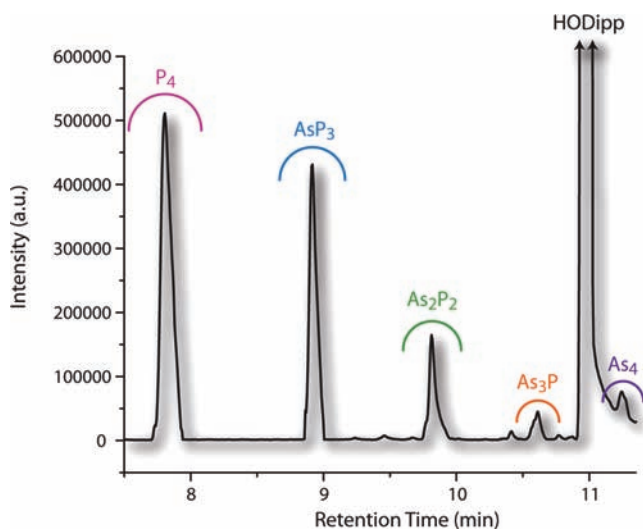


Figure 7. GC–MS chromatogram following treatment of *in situ* generated 6-P₃, 6-AsP₂, 6-As₂P, and 6-As₃ with AsCl₃. P₄ added as an internal standard.

concentration of the unexpected 6-As₂P (and from subsequent analysis, *vide infra*), we propose that 6-As₃ is also present in low concentration. Treatment of this crude reaction mixture with AsCl₃ with the exclusion of light rapidly generated a reaction mixture containing Cl₂Nb(ODipp)₃(THF) and the tetraatomic interpnictides AsP₃, As₂P₂, As₃P, as well as As₄ (Scheme 6).⁶⁰ The presence of the four tetrahedral molecules is confirmed by ³¹P NMR spectroscopy and by GC–MS (Table 4, Figure 7 and Figures 8S–13S, Supporting Information). It is of note that the

(60) P₄ was used as an internal standard for monitoring purposes. No P₄ was present in the reaction mixture prior to its addition.

ratio of As to P atoms in the final product mixture is 1 to 1.6, which is very near the 1 to 1.3 ratio that we would expect (3/4 AsP₃ + AsCl₃) over the course of the two reactions. This is an important observation that implies that there is no selective loss of As or P atoms during the synthesis. We are currently investigating alternative syntheses of As₂P₂ and As₃P for exploration of these molecules as pure substances.

Conclusions and Future Directions

For the first time, the reaction chemistry of the interpnictide compound AsP₃ has been investigated. In the presence of Lewis acidic metal fragments, adduct formation is selective for binding at a single phosphorus vertex, and reducing main group and transition metal species effect radical cleavage reactions where a single As–P bond is selectively cleaved. Furthermore, AsP₃ can be used to prepare otherwise difficult to access mixed As/P molecules, both as free entities, in the case of the mixed interpnictides As_nP_{4–n} (*n* = 1–3), or as coordinated ligands, in the case of 4-AsP. The electronic and structural features that render AsP₃ distinct from P₄ are consistent with the reactivity patterns that have emerged. In particular, we have been able to distinguish between the vertices of the AsP₃ molecule in the formation of compounds 1 and 2. DFT calculations have provided us insight into the electronic structure of this unique tetraatomic molecule and have provided us with estimates of important thermodynamic parameters. We are currently investigating the use of AsP₃ in the synthesis of solid-state, mixed arsenide-phosphide materials as well as a “red AsP₃” phase, both of which may be of interest for the development of novel semiconductor materials. Future work will target the directed synthesis of the new interpnictides As₂P₂ and As₃P reported herein as well as further unveil the diverse reaction chemistry of AsP₃.

Experimental Details

General Considerations. All manipulations were performed in a Vacuum Atmospheres model MO-40 M glovebox under an inert atmosphere of purified N₂. All solvents were obtained anhydrous and oxygen-free by bubble degassing (N₂) and purification through columns of alumina and Q5. Deuterated solvents were purchased from Cambridge Isotope Laboratories. Benzene-*d*₆ and toluene-*d*₈ were degassed and stored over molecular sieves for at least 2 d prior to use. Celite 435 (EM Science) were dried by heating above 200 °C under a dynamic vacuum for at least 24 h prior to use. AsP₃,³ Mo(N[^tBu]Ar)₃,⁶¹ Ti(N[^tBu]Ar)₃,⁴⁰ Cl₂Nb(ODipp)₃,⁵⁹ Nb(H)(η^2 -^tBu(H)C=NAr)(N[CH₂^tBu]Ar)₂ (PN(ⁱPr)₂N(SiMe₃)₂),³⁸ and FeCp*(dppe)Cl³⁷ were synthesized according to reported methods. All glassware was oven-dried at temperatures greater than 170 °C prior to use. NMR spectra were obtained on Varian Inova 500 instruments equipped with Oxford Instruments superconducting magnets and referenced to residual C₆D₆ (¹H = 7.16 ppm, ¹³C = 128.06 ppm) or (CD₃)₂CO (¹H = 2.05 ppm, ¹³C = 29.84 ppm). ³¹P NMR spectra were referenced externally to 85% H₃PO₄ (0 ppm). Elemental analyses were performed by Midwest Microlab LLC, Indianapolis, IN. UV–vis spectra were obtained on a Hewlett-Packard 845x series UV–vis system equipped with a tungsten lamp. GC–MS data were collected using an Agilent 6890N network GC system with an Agilent 5973 Network mass selective detector and an Rtx-1 column from Restek. MALDI-TOF MS data were collected on a Bruker OmniFlex instrument, and data were processed using the Bruker FlexControl software package. For

(61) Laplaza, C. E.; Cummins, C. C. *Science* **1995**, *268*, 861–863.

(62) Figueroa, J. S.; Cummins, C. C. *J. Am. Chem. Soc.* **2003**, *125*, 4020–4021.

(63) Sheldrick, G. M. *SADABS*; Bruker AXS Inc.: Madison, WI, 2005.

Raman studies, an Invictus solid-state laser at 785 nm, manufactured by Kaiser Optics, was routed through fiber-optic cables to a Hololab series 5000 Raman Microscope. The Raman scattering was observed via 180° reflectance through the objective of the Raman microscope. Each spectrum was corrected for dark current and cosmic ray interference using the Hololab software. Powder diffraction data were collected on a PANalytical X'Pert Pro multipurpose diffractometer equipped with a 1.8 kW sealed tube X-ray source using Mo K α radiation ($\lambda = 0.71073 \text{ \AA}$) and equipped with high-speed Bragg–Brentano optics. Scanning electron microscopy was performed on a JEOL JSM-5910 instrument using a JEOL BEI detector and a Rontec EDX system for elemental analysis and mapping.

Thermolysis of AsP₃. AsP₃ (100 mg) was loaded into a thick-walled glass tube. The tube was sealed under vacuum. The tube was wired to a thermocouple probe, and the probe and tube were wrapped completely with heating tape. The heating tape was set to heat at 290–300 °C for 40 h. After this time the apparatus was cooled, and the heating tape was removed. The white-yellow AsP₃ had been converted to a red-black material as well as a metallic shiny material which had sublimed partially up the tube. Raman spectroscopy of the bulk material through the tube revealed complete consumption of the AsP₃ tetrahedron. The tube was scored and broken open. The contents of the tube were removed and placed on a zero background silicon 510 surface for powder diffraction. Powder diffraction data: broad peaks centered around 18°, 32°, 58°, and 90° 2 θ . The product mixture was then also analyzed by Raman spectroscopy and EDS using a JEOL SEM microscope. Raman spectroscopy results: broad and weak resonance at 280 cm⁻¹, sharp and intense resonance at 320 cm⁻¹, broad and intense resonances extending from 340 to 500 cm⁻¹. SEM data: in a 50 $\mu\text{m} \times 50 \mu\text{m}$ region, elemental composition analysis gave phosphorus 74.01% (error 0.66%) and arsenic 25.98% (error 0.76%).

[(AsP₃)FeCp*(dppe)][BPh₄], 1. FeCp*(dppe)Cl (144 mg, 0.230 mmol, 1 equiv) was dissolved in 8 mL of THF and was transferred to a vial containing solid AsP₃ (43 mg, 0.256 mmol, 1.1 equiv) and a stir bar. The reaction mixture was allowed to stir for 30 min during which time the originally green reaction mixture went slightly orange (subtle change). At this point NaBPh₄ (79 mg, 0.230 mmol, 1 equiv) was added, resulting in immediate formation of a bright magenta-purple color. The reaction mixture was allowed to stir an additional 10 min. At this point the reaction mixture was concentrated, and *n*-pentane was added to help precipitate the salt. The reaction mixture was filtered through a plug of Celite, and the volatile components were concentrated to 5 mL. Et₂O (3 mL) was added, and the purple solution was placed in the -35 °C freezer to induce precipitation. After 30 min, a copious magenta precipitate had formed. This precipitate was isolated atop a frit, resulting in 198 mg (0.183 mmol) of material (80% yield). X-ray diffraction-quality crystals were grown from an Et₂O/CH₂Cl₂ (1:1) solution at -35 °C. ¹H NMR (20 °C, acetone-*d*₆, 500 MHz): $\delta = 1.48$ (15H, s, Cp*-Me), 2.61 (2H, m, dppe-CH₂), 2.75 (2H, m, dppe-CH₂), 6.77 (m, 8H, Ar), 6.91 (m, 12H, Ar), 7.34 (br, 8H, Ar), 7.50 (br, 4H, Ar), 7.61 (br, 8H, Ar). ³¹P{¹H} NMR (20 °C, acetone-*d*₆, 202.5 MHz): $\delta = -450$ (2P, d, ¹J = 245 Hz, non-Fe bound P), -261 (1P, tt, ¹J = 245 Hz, ²J = 37 Hz, Fe-bound P), 89 (2P, d, ²J = 37 Hz, dppe-P). ¹³C{¹H} NMR (20 °C, acetone-*d*₆, 125.8 MHz): $\delta = 10.6$ (s, Cp*-Me), 29.5 (m, dppe-CH₂), 90.7 (s, Cp*-ring), 122.8 (Ar), 126.6 (Ar), 129.6 (Ar), 131.7 (Ar), 133.2 (Ar), 137.6 (Ar), 164.9 (Ar), 165.7 (Ar). UV-vis: 494 nm (ϵ 590 M⁻¹ cm⁻¹), 543 nm (ϵ 480 M⁻¹ cm⁻¹). MALDI-TOF MS: 757.0318 *m/z* [(AsP₃)FeCp*(dppe)]⁺, 589.2216 *m/z* [(FeCp*(dppe)]⁺, 319.1650 *m/z* [BPh₄]⁻. Elem. Anal. Calcd for C₆₀H₅₉AsBF₄P₅: C 66.94, H 5.52, P 14.39; Found: C 66.87, H 5.61, P 13.98.

AsP₃(P(N(Pr)₂)N(SiMe₃)₂), 2. (P(N(Pr)₂)N(SiMe₃)₂) (190 mg, 0.295 mmol) was dissolved in 10 mL of toluene and was added slowly to a vial containing a solution of AsP₃ (54 mg, 0.321 mmol) in 5 mL of toluene. Upon mixing the two colorless reagents, the reaction mixture took on a vibrant yellow color. The mixture was stirred for an additional 20 min, and an aliquot was withdrawn for

NMR analysis which showed clean and complete conversion of the starting materials to AsP₃(P(N(Pr)₂)N(SiMe₃)₂). The reaction mixture was taken to dryness under reduced pressure, and the resulting residue was dissolved in *n*-hexane/Et₂O (2:1) and recrystallized, affording 196 mg (0.261 mmol, 88% yield) of pale-yellow crystals of AsP₃(P(N(Pr)₂)N(SiMe₃)₂) (mixture of diastereomers). ¹H NMR (20 °C, benzene-*d*₆, 500 MHz): $\delta = 0.43$ (36H, br, SiMe₃), 1.03 (12H, m, Pr-Me), 1.20 (6H, m, Pr-Me), 1.26 (6H, m, Pr-Me), 3.34 (2H, m, Pr-CH), 3.48 (2H, m, Pr-CH). ³¹P{¹H} NMR (20 °C, benzene-*d*₆, 202.5 MHz): $\delta = -311$ (2P, m, P(PP)As), -148.5 (1P, m, P(PP)As), 118.5 (1P, m, As bound phosphine), 123 (1P, m, P bound phosphine). ¹³C{¹H} NMR (20 °C, benzene-*d*₆, 125.8 MHz): $\delta = 5.1$ (br, SiMe₃), 6.53 (br, SiMe₃), 23.6 (m, Pr-Me), 24.7 (m, Pr-Me), 48.2 (m, Pr-CH). Elem. Anal. Calcd for C₂₄H₆₄AsN₄P₅Si₄: C 38.39, H 8.59, N 7.46, P 20.62; Found: C 39.42, H 8.78, N 8.26, P 19.27.

Treatment of AsP₃ (and P₄) with Ti(N[^tBu]Ar)₃, Synthesis of 3-P₄ and 3-AsP₃. To begin the measurements, AsP₃ (15 mg, 0.09 mmol), P₄ (11 mg, 0.09 mmol), PPh₃ (12 mg, 0.045 mmol), Ti(N[^tBu]Ar)₃ (68 mg, 0.118 mmol), and toluene (872 mg) were combined and placed in a J-Young-style NMR tube. The temperature was varied between 5 and 35 °C, allowing the tube to fully equilibrate before taking the final concentration readings. The simplest equilibrium expression was not obeyed, but the product concentration for 3-AsP₃ was always higher than for 3-P₄. For example, at 20 °C 3-AsP₃ and 3-P₄ were present in a 7:1 ratio (Figure 14S, Supporting Information). These results show that in a 1:1 mixture of AsP₃ and P₄, a greater percentage of AsP₃ undergoes reaction. This experiment was repeated with only AsP₃ in the reaction mixture and alternatively with only P₄ present to obtain clean NMR spectral data for both 3-AsP₃ and 3-P₄. ³¹P{¹H} NMR (AsP₃[Ti(N[^tBu]Ar)₃], 20 °C, benzene-*d*₆, 202.5 MHz): $\delta = -275$ (2P, d, ¹J = 200 Hz, P(PP)As), -9.6 (1P, t, ¹J = 200 Hz, P(PP)As). ³¹P{¹H} NMR (P₄[Ti(N[^tBu]Ar)₃], 20 °C, benzene-*d*₆, 202.5 MHz): $\delta = -284$ (2P, t, ¹J = 188 Hz, P(PP)P), 12.9 (2P, t, ¹J = 188 Hz, P(PP)P).

Treatment of AsP₃ with Nb(H)(η^2 -^tBu(H)C=NAr)(N[CH₂^tBu]Ar)₃, Synthesis of 4-AsP and 4-P₂. Nb(H)(η^2 -^tBu(H)C=NAr)(N[CH₂^tBu]Ar)₂ (113 mg, 0.17 mmol) was dissolved in 5 mL of Et₂O and was added to a vial containing AsP₃ (10 mg, 0.06 mmol) and a stir bar. The reaction mixture was vigorously stirred for 90 min during which time the originally yellow solution took on a deep-green color. The volatile components of the reaction mixture were removed under reduced pressure. The resulting green powder was taken up in C₆D₆ for NMR analysis. Recrystallization from Et₂O/C₅ (1:2) afforded 98 mg (82% yield) of a 1:1 mixture of (μ_2 : η^2 : η^2 -P₂)[Nb(N[CH₂^tBu]Ar)₃]₂ and (μ_2 : η^2 : η^2 -AsP)[Nb(N[CH₂^tBu]Ar)₃]₂. ¹H NMR (20 °C, benzene-*d*₆, 500 MHz): $\delta = 6.98$ (24H, br, o-Ar), 6.59 (12H, s, p-Ar), 4.23 (24H, br, N-CH₂), 2.25 (36H, s, Ar-CH₃, μ_2 -P₂), 2.23 (36H, s, Ar-CH₃, μ_2 -AsP), 0.97 (54H, s, ^tBu, μ_2 -P₂), 0.95 (54H, s, ^tBu, μ_2 -AsP). ³¹P{¹H} NMR (20 °C, benzene-*d*₆, 202.5 MHz): $\delta = 399$ (2P, br, μ_2 -P₂), 438 (1P, br, μ_2 -AsP). ¹³C{¹H} NMR (20 °C, benzene-*d*₆, 125.7 MHz): $\delta = 154.2$ (Ar), 138.1 (Ar), 126.6 (Ar), 124.4 (Ar), 73 (N-CH₂), 37.3 (C(CH₃)), 30.3 (C(CH₃), μ_2 -P₂), 30.1 (C(CH₃), μ_2 -AsP), 22.1 (Ar-CH₃).

Treatment of AsP₃ with Mo(N[^tBu]Ar)₃, Synthesis of 5-As and 5-P. Mo(N[^tBu]Ar)₃ (100 mg, 0.16 mmol) was dissolved in 5 mL of Et₂O and was added to a vial containing solid AsP₃ (8 mg, 0.047 mmol). The mixture was stirred for 60 min during which time the reaction mixture assumed a dark-orange color. The volatile components of the reaction mixture were removed under reduced pressure. The resulting residue was dissolved in C₆D₆ and was taken for NMR analysis. Recrystallization from Et₂O/*n*-pentane (1:2) afforded 75 mg (70% yield) of 3:1 PMo(N[^tBu]Ar)₃ and AsMo(N[^tBu]Ar)₃. ¹H NMR (20 °C, benzene-*d*₆, 500 MHz): $\delta = 6.61$ (6H, s, o-Ar), 5.81 (3H, br, p-Ar), 2.04 (18H, s, Ar-Me), 1.66 (27H, s, ^tBu). ³¹P{¹H} NMR (20 °C, benzene-*d*₆, 202.5 MHz): $\delta = 1216$ (1P, br, P=Mo). ¹³C{¹H} NMR (20 °C, benzene-*d*₆, 125.7 MHz): $\delta = 150.6$ (Ar, P=Mo), 150.0 (Ar, As=Mo), 136.85 (Ar, P=Mo),

136.80 (Ar, As≡Mo), 130.6 (Ar, As≡Mo), 130.4 (Ar, P≡Mo), 127.7 (Ar), 60.6 (C(CH₃), P≡Mo), 59.8 (C(CH₃), As≡Mo), 34.1 (C(CH₃), As≡Mo), 33.9 (C(CH₃), P≡Mo), 21.5 (Ar-CH₃).

Reduction of Cl₂Nb(ODipp)₃ in the Presence of AsP₃ and Na/Hg Followed by Treatment with AsCl₃, Generation of 6-P₃, 6-AsP₂, 6-As₂P, 6-As₃, AsP₃, As₂P₂, As₃P, and As₄. Cl₂Nb(ODipp)₃ (278 mg, 0.40 mmol) was combined with solid AsP₃ (67 mg, 0.40 mmol) and then dissolved in 10 mL of THF. After all the AsP₃ was dissolved a 0.5% Na/Hg amalgam was added. The reaction mixture was allowed to stir for 20 min during which time it assumed a dark orange-brown color. The reaction mixture was taken to dryness. To the residue was added 5 mL of Et₂O. The resulting residue was filtered to remove any insoluble material. The filtrate was taken to dryness under reduced pressure. The resulting residue was dissolved in a stock solution of P₄ (0.158 mmol total as an internal standard) in C₆D₆ for NMR analysis. ³¹P NMR (20 °C, benzene-*d*₆, 202.5 MHz): δ = -520 (P₄, s, 0.1581 mmol), -206 ([Na][P₃Nb(ODipp)₃], s, 0.1935 mmol, 48% yield), -167 ([Na][P₂-AsNb(ODipp)₃], s, 0.090 mmol, 23% yield), -132 ([Na][PAs₂-Nb(ODipp)₃], s, 0.0198 mmol, 5% yield). The total yield of 6-P₃, 6-AsP₂, and 6-As₂P is 76% based on Cl₂Nb(ODipp)₃, which is consistent with the yields obtained for the synthesis of 6-P₃ from P₄.³ The NMR tube was returned to the glovebox, and its contents were taken to dryness. The resulting residue was dissolved in 5 mL of THF, and the solution was frozen in the cold well. AsCl₃ (72 mg) was added to this thawing solution (as a stock solution in toluene). The resulting mixture was allowed to stir for 20 min after which time it was filtered through a pad of Celite and concentrated to 1 mL. This sample was placed in an NMR tube (wrapped in Al foil) for analysis. ³¹P{¹H} NMR (20 °C, benzene-*d*₆, 202.5 MHz): δ = -520 (P₄, s), -484 (AsP₃, s), -452 (As₂P₂, s), -432 (AsP₃, s). A portion of the sample was diluted 100-fold with C₆H₆ and was analyzed by GC-MS. GC-MS: P₄ [retention time 7.8 min, parent ion 124 *m/z* with fragments at 93 (P₃) and 62 (P₂), total area 50994], AsP₃ [retention time 8.9 min, parent ion 168 *m/z* with fragments at 137 (AsP₂), 106 (AsP), 93 (P₃), 75 (As), and 62 (P₂), total area 30475, 49% yield from 6-P₃], As₂P₂ [retention time 9.8 min, parent ion 212 *m/z* with fragments at 181 (As₂P), 150 (As₂), 137 (AsP₂), 106 (AsP), 75 (As), and 62 (P₂), total area 11348, 39% yield from 6-AsP₂], As₃P [retention time 10.6 min, parent ion 256 *m/z* with fragments at 225 (As₃), 181 (As₂P), 150 (As₂), 106 (AsP), and 75 (As), total area 3176, 50% yield from 6-As₂P], As₄ [retention time 11.2 min, parent ion 300 *m/z* with fragments at 150 (As₂) and 75 (As); peaks from neighboring HODipp signal also present, approximate total area 1977, 2% yield from Cl₂Nb(ODipp)₃].

X-ray Diffraction Studies. Diffraction-quality crystals of [(AsP₃)FeCp*(dppe)][BPh₄] were grown from CH₂Cl₂/Et₂O at -35 °C over the course of several days. Diffraction-quality crystals of AsP₃(P(N(Pr)₂)N(SiMe₃)₂)₂ were grown from *n*-hexane/Et₂O by cooling at -35 °C over the course of two days. The crystals were mounted in hydrocarbon oil on a nylon loop. Low-temperature (100 K) data were collected on a Siemens Platform three-circle diffractometer coupled to a Bruker-AXS Smart Apex CCD detector with graphite-monochromated Mo K α radiation ($\lambda = 0.71073$ Å) performing φ and ω scans. A semiempirical absorption correction was applied to the diffraction data using SADABS.⁶³ The structures were solved by direct methods using SHELXS⁶⁴ and refined against *F*² on all data by full-matrix least-squares with SHELXL-97.⁶⁵ All non-H atoms were refined anisotropically. All H atoms were included in the models at geometrically calculated positions and refined using a riding model. The isotopic displacement parameters of all H atoms were fixed to 1.2 times the *U* value of the atoms

they are linked to (1.5 times for methyl groups). All disorders were refined within SHELXL with the help of rigid bond restraints as well as similarity restraints on the anisotropic displacement parameters for neighboring atoms and on 1,2- and 1,3-distances throughout the disordered components. The relative occupancies of disordered components were refined freely within SHELXL. Further details are available in the Supporting Information (Table S1 and a CIF file) and from the CCDC under deposition numbers 730555 (2) and 730556 (1).

Computational Studies. All calculations were carried out using ADF 2008.01 from Scientific Computing and Modeling (<http://www.scm.com>)^{20,21} on a 32-processor Quantum Cube workstation from Parallel Quantum Solutions (<http://www.pqs-chem.com>). All of the calculations were repeated using the OLYP functionals which are a combination of the OPTX exchange functional of Handy and Cohen used with Lee, Yang, and Parr's nonlocal correlation function (LYP).⁶⁶⁻⁶⁸ In addition, all calculations were carried out using the zero-order regular approximation (ZORA) for relativistic effects.⁶⁹⁻⁷¹ The basis sets used were quadruple- ζ with four polarization functions (QZ4P) for As and P in the calculation of E₄ tetrahedra (E = As, P) and triple- ζ with two polarization functions (TZ2P) for all other calculations, as supplied with ADF. Chemical shielding tensors were calculated for the ³¹P nuclei in the optimized structures by the GIAO method using the ADF package.⁷²⁻⁷⁵ The functionals, basis sets, and relativistic approximations used were the same as those described above. The isotropic value of the chemical shielding was converted to a chemical shift downfield of 85% phosphoric acid using P₄, white phosphorus, as a computational reference; the computed absolute shielding value of P₄ was correlated with a chemical shift equal to its experimental value (-520 ppm) in dilute benzene solution.⁷⁶ For zero-point energy corrections, frequencies calculations were computed using optimized structures as described above.

Acknowledgment. We thank the NSF (Grant CHE-719157) and ThermPhos International for generous funding and support for this project.

Supporting Information Available: Full crystallographic data on compounds 1 and 2, complete ADF output files, and phosphorus NMR spectra for all reactions. This material is available free of charge via the Internet at <http://pubs.acs.org>.⁷⁷

JA906294M

- (64) Sheldrick, G. M. *Acta Crystallogr., Sect. A* **1990**, *A46*, 467-473.
 (65) Sheldrick, G. M. *SHELXL-97: Program for crystal structure determination*; University of Göttingen: Göttingen, Germany, 1997.
 (66) Lee, C.; Yang, W.; Parr, R. G. *Phys. Rev. B* **1988**, *37*, 785-789.
 (67) Handy, N. C.; Cohen, A. J. *Mol. Phys.* **2001**, *99*, 403-412.
 (68) Baker, J.; Pulay, P. *J. Comput. Chem.* **2003**, *24*, 1184-1191.
 (69) van Lenthe, E.; Baerends, E. J.; Snijders, J. G. *J. Chem. Phys.* **1993**, *99*, 4597-4610.
 (70) van Lenthe, E.; Ehlers, A.; Baerends, E. J. *J. Chem. Phys.* **1999**, *110*, 8943-8953.
 (71) van Lenthe, E.; Baerends, E.; Snijders, J. G. *J. Chem. Phys.* **1994**, *101*, 9783-9792.
 (72) Schreckenbach, G.; Ziegler, T. *J. Phys. Chem.* **1995**, *99*, 606-611.
 (73) Schreckenbach, G.; Ziegler, T. *Int. J. Quantum Chem.* **1997**, *61*, 899-918.
 (74) Wolff, S. K.; Ziegler, T. *J. Chem. Phys.* **1998**, *109*, 895-905.
 (75) Wolff, S. K.; Ziegler, T.; van Lenthe, E.; Baerends, E. J. *J. Chem. Phys.* **1999**, *110*, 7689-7698.
 (76) van Wullen, C. *Phys. Chem. Chem. Phys.* **2000**, *2*, 2137-2144.
 (77) CIF files are available from the Cambridge Crystallographic Database under deposition numbers 730555 (2) and 730556 (1).